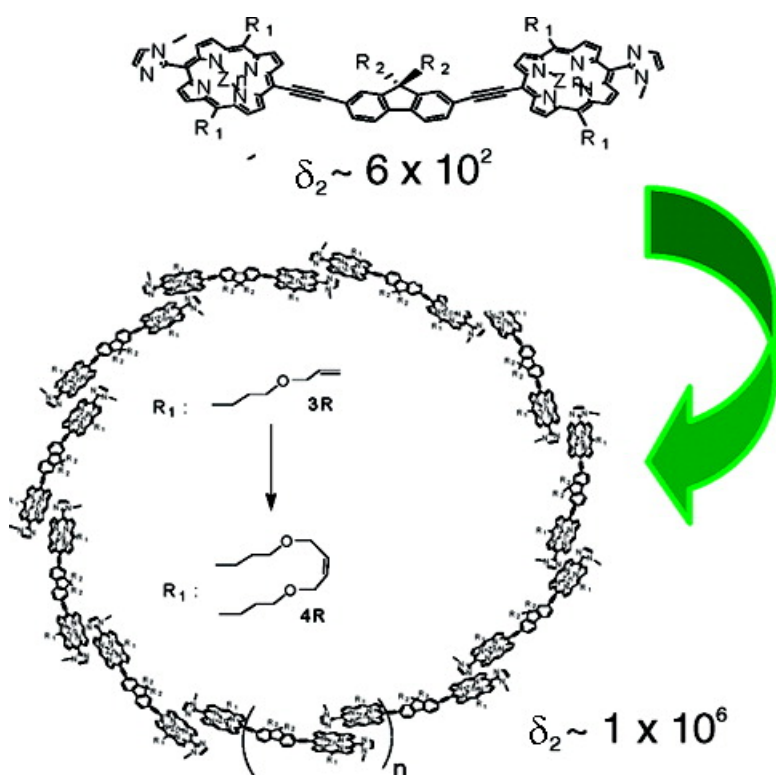


## Synthesis and Two-Photon Absorption Enhancement of Porphyrin Macrocycles

Jeffery E. Raymond, Ajit Bhaskar, Theodore Goodson III, Naoyuki Makiuchi, Kazuya Ogawa, and Yoshiaki Kobuke

*J. Am. Chem. Soc.*, **2008**, 130 (51), 17212-17213 • DOI: 10.1021/ja804415b • Publication Date (Web): 02 December 2008

Downloaded from <http://pubs.acs.org> on February 8, 2009



### More About This Article

Additional resources and features associated with this article are available within the HTML version:

- Supporting Information
- Access to high resolution figures
- Links to articles and content related to this article

- Copyright permission to reproduce figures and/or text from this article

[View the Full Text HTML](#)



## Synthesis and Two-Photon Absorption Enhancement of Porphyrin Macrocycles

Jeffery E. Raymond,<sup>†</sup> Ajit Bhaskar,<sup>†</sup> Theodore Goodson III,<sup>\*,†</sup> Naoyuki Makiuchi,<sup>‡</sup> Kazuya Ogawa,<sup>\*,‡</sup> and Yoshiaki Kobuke<sup>\*,‡</sup>

Department of Chemistry, Department of Macromolecular Science and Engineering, University of Michigan, Ann Arbor, Michigan 48109 and Graduate School of Materials Science, Nara Institute of Science and Technology, 8916-5 Takayama, Ikoma, Nara 630-0101

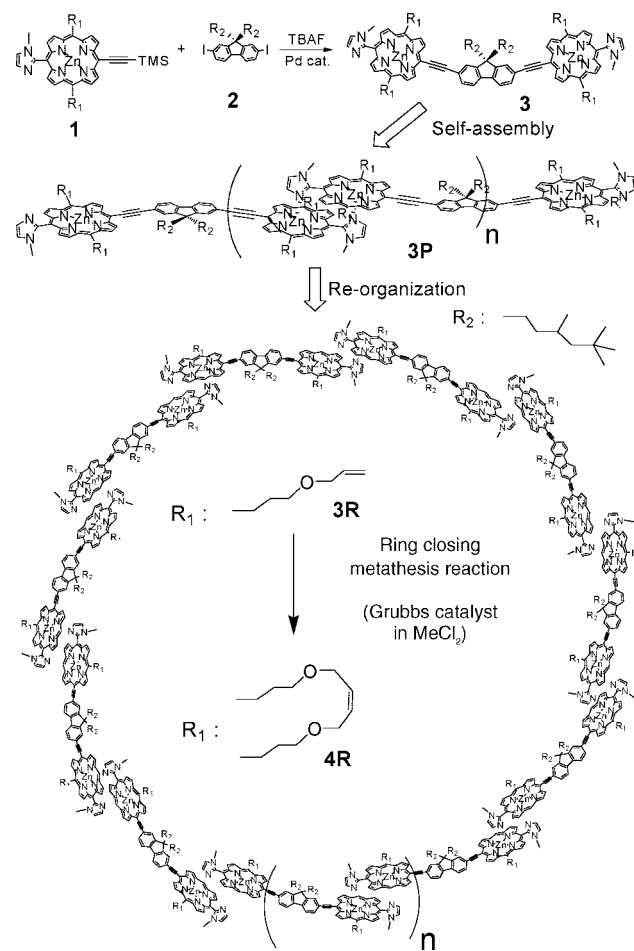
Received June 11, 2008; E-mail: tgoodson@umich.edu; oga@ms.naist.jp; kobuke@ms.naist.jp

It is now clear that dendrimers, 2-D arrays, and macrocycles offer new and enhanced effects for nonlinear and quantum optical applications.<sup>1,2</sup> There is still a need to create superior self-assembled materials as building blocks for novel optical applications. New variations of the porphyrin molecule have recently been generated for this purpose. There have been reports of the use of porphyrins in polymers, linear arrays, dendrimers, and, in this report, cyclic aggregates.<sup>3</sup> In particular, it would be interesting to know the effect of the number of porphyrin dimer units in cyclic geometries on the two-photon cross section ( $\delta_2$ ). There is a large degree of interest in materials with large  $\delta_2$  values in the 700–900 nm range, a region where porphyrin assemblies have great promise. Indeed, for the porphyrin macrocycles in this report,  $\delta_2$  values in this critical region are observed to be as high as  $1.0 \times 10^6$  GM.

The bisporphyrin dimer **3** was synthesized from ethynylimidazolyloporphyrin **1** and 2,7-diiodofluorene **2** using a Pd<sub>2</sub>(dba)<sub>3</sub>/AsPh<sub>3</sub> catalytic system at 24% yield. When **3** was dissolved in a nonpolar solvent, chloroform, the long linear polymer **3P** first formed by self-coordination. **3P** was gradually converted to smaller cyclic arrays (**3R**) through a reorganization process at 45 °C,<sup>4</sup> eventually converging to a mixture with a distribution maximum close to  $3 \times 10^4$  Da (Supporting Information). To determine the exact molecular weights of the arrays by mass measurement, the coordination between dimers was fixed via a ring-closing metathesis reaction of meso-substituents to produce **4R**.<sup>6</sup> After the reaction, GPC separation was performed, and the fractions were subjected to MALDI-TOF measurements. The bulk solution was found to contain several sizes of macrocycles, with the 11-mer ( $n = 1$ ) through the 19-mer ( $n = 9$ ) being separated into distinct fractions (Supporting Information). Molecular modeling, by way of a MOPAC calculation, found that the 17-mer and 18-mer macrocycles should be the cyclic species which contain the least amount of ring strain.

Steady-state absorption investigations (Figure 1) for these systems show a significant red shift in the Soret band ( $\sim 25$  nm) and a slightly less pronounced red shift ( $\sim 20$  nm) in the Q-band for all of the macrocycles in comparison to the dimer. The distinct broadening of the Soret band seen is typical of other porphyrin assemblies. There is a significant decrease in quantum yield when transitioning from the lone dimer to the macrocycle species though the macrocycles still possess quantum yields comparable to previously investigated porphyrin polymers and macrocycles.<sup>3–5</sup> This is expected because of the arrangement of the porphyrins and slight disruption of resonance at the covalent linkage points. For smaller rings, since the acetylene bridge is less stressed than that of the porphyrin or fluorene regions, the strain at these bonds will be greater, leading to lower quantum yields.

**Scheme 1.** Synthesis of a Covalently Bonded Porphyrin Macrocycle by a Self-Assembly Pathway



The weakening of the planarity at the acetylenic regions is observed as a slight blue-shift in the Q-band absorption in the macrocycle systems, when smaller rings are compared to the less strained 17-mer species.<sup>5c,d</sup> The subsequent increase in quantum yield ( $\eta$ ), as the size of the macrocycle goes from an 11-mer to the 17-mer, confirms that the less distorted system sees less fluorescence inhibition. The 19-mer in turn sees another  $\eta$  decrease as the size and flexibility of the macrocycle becomes such that folding and bending of the macrocycle allows for even further distortion at acetylenic linkages and a greater number of intermolecular quenching sites within the molecule.

A summary of the two-photon properties and quantum yields for the system studied are given in Table 1. The two-photon

<sup>†</sup> University of Michigan.

<sup>‡</sup> Nara Institute of Science and Technology.

**Table 1.** TPA and TPEF Enhancement in Porphyrin Macrocycles<sup>a</sup>

porphyrin	dimer number	total $\delta$ (GM)	$\delta$ /dimer (GM)	$\eta$	$\eta\delta$ /dimer (GM)
dimer	1	572	572	0.342	196
$n = 1$ ( <b>4R</b> )	11	$4.1 \times 10^5$	$3.7 \times 10^4$	0.026	969
$n = 3$ ( <b>4R</b> )	13	$5.1 \times 10^5$	$3.9 \times 10^4$	0.034	1342
$n = 7$ ( <b>4R</b> )	17	$6.8 \times 10^5$	$4.0 \times 10^4$	0.044	1763
$n = 9$ ( <b>4R</b> )	19	$1.0 \times 10^6$	$5.3 \times 10^4$	0.017	894

<sup>a</sup> GM =  $10^{-50}$  cm<sup>4</sup> s/photon.

absorption and emission properties of this system were investigated by the TPEF method with  $\sim 100$  fs pulses as outlined elsewhere in our previous reports.<sup>1,2</sup> The dimer in this investigation shows only a small 2P response when considered in isolation. However, upon cyclization and subsequent covalent linkage, a 2 order of magnitude increase in  $\delta_2$  and an order of magnitude increase in the two-photon fluorescence signal was observed. Though the acetylinic bridging between dimer units is not assumed to contribute to the two-photon cross section of the macrocycle implicitly, they are assumed to prevent dissociation of the imidazolyl linkages and make the assemblies more viable for use in a wider assortment of environments.

The  $\delta_2$  for the cyclized systems is given in Figure 2. For these systems it was found that the maximum two-photon cross sections occurred near 830 nm. It was also found that for cyclized porphyrin macromolecules the increased ring size leads to an increased dimer cross section, making the 19-mer a preferred candidate for TPA applications. This is one of the largest cross sections reported for porphyrin systems on the femtosecond time scale.<sup>3–5</sup> The maximum TPEF is attributed to the macrocycle with the lowest strain at its linkage points, the 17-mer, and is also one of the largest values reported for porphyrin system at a  $\delta_2 \times \eta$  value of  $1.8 \times 10^3$  GM per dimer.

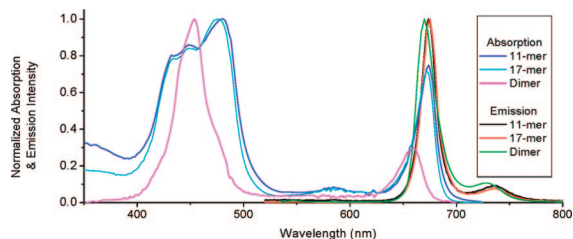


**Figure 1.** Steady-state absorption and emission data for porphyrin macrocycles. A red shift in the absorption (20–25 nm) is seen in the porphyrin macrocycles when compared to the dimer. Only selected spectra are presented for clarity.

The  $\delta_2$  enhancement seen in these macrocycles was attributed to several distinct factors. The complementary coordination of the imidazolyl group to the neighboring porphyrin's Zn(II) enhances the local dipole–dipole interaction in the macrocycle.<sup>3,6</sup> In forming cyclized molecules with covalent links preventing dissociation, we effectively enforce a minimal amount of variation in the coplanarity and distance between porphyrin rings with a rigid spacing unit between bound chromophores.<sup>7</sup> This binding in effect leads to lower dihedral angle disruption between the porphyrin units and fluorene and higher dimer symmetry.<sup>5d</sup> All of these properties have been shown to contribute to strongly cooperative intramolecular interactions in multichromophore arrays and provide precedence for the enhanced  $\delta_2$  observed in this TPEF study.

In this study we show that by an elegant combination of self-assembly and a metathesis ring closing reaction, large porphyrin

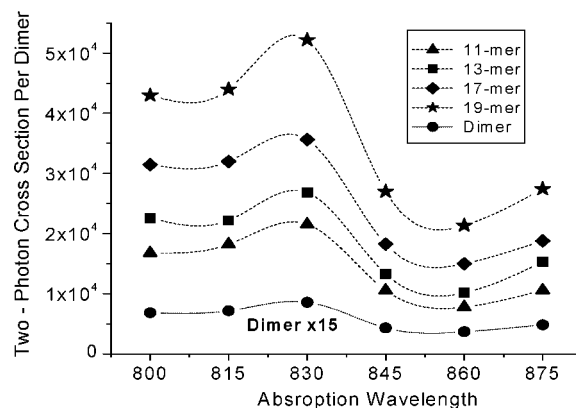


**Figure 2.** Two-photon cross section spectra per dimer unit for the porphyrin macrocycles studied. The dimer is shown at 15 times its actual value for contrast.

macrocycles can be generated and separated by size. An increase of 2 orders of magnitude for the  $\delta_2$  per dimer unit was observed in these porphyrin macromolecules. The macrocycles have greater promise for two-photon applications in multiple solvents and at wider pH ranges than aggregates which lack covalent bonds. These materials provide greater 2P response than linear counterparts, showing potential for use in both TPA and TPEF applications and providing a new avenue from which to probe porphyrin dimer–dimer interactions and flexible covalent bridges in imidazolyl–Zn(II) porphyrin systems.

**Acknowledgment.** Support for this project was provided by NSF-DMR-Polymers.

**Supporting Information** Detailed experimental procedures and associated spectrometric data (PDF). This material is available free of charge via the Internet at <http://pubs.acs.org>.

## References

- (a) Williams-Harry, M.; Bhaskar, A.; Ramakrishna, G.; Goodson, T., III; Imamura, M.; Mawatari, A.; Nakao, K.; Enozawa, H.; Nichinaga, T.; Iyoda, M. *J. Am. Chem. Soc.* **2008**, *130*, 3252–3253. (b) Bhaskar, A.; Ramakrishna, G.; Lu, Z.; Twieg, R.; Hales, J.; Hagan, D.; Stryland, E.; Goodson, T., III *J. Am. Chem. Soc.* **2006**, *128*, 11840–11849. (c) Ispasoiu, R.; Balogh, L.; Varnavski, O.; Tomalia, D.; Goodson, T., III *J. Am. Chem. Soc.* **2000**, *122*, 11005–11006. (d) Bhaskar, A.; Ramakrishna, G.; Hagedorn, K.; Varnavski, O.; Mena-Osteritz, E.; Bauerle, P.; Goodson, T., III *J. Phys. Chem. B* **2007**, *111*, 946.
- (a) Ramakrishna, G.; Bhaskar, A.; Bauerle, P.; Goodson, T., III *J. Phys. Chem. A* **2008**, *112* (10), 2018–2026. (b) Bhaskar, A.; Guda, R.; Haley, M. M.; Goodson, T. G., III *J. Am. Chem. Soc.* **2006**, *128*, 13972. (c) Goodson, T., III *Acc. Chem. Res.* **2005**, *38*, 99–107.
- (a) Ogawa, K.; Ohashi, A.; Kobuke, Y.; Kamada, K.; Ohta, K. *J. Am. Chem. Soc.* **2003**, *125*, 13356. (b) Ogawa, K.; Ohashi, A.; Kobuke, Y.; Kamada, K.; Ohta, K. *J. Phys. Chem. B* **2005**, *109*, 22003. (c) Lee, D.-I.; Goodson, T., III *J. Phys. Chem. B* **2006**, *110*, 25582–25585. (d) Drobizhev, M.; Stepanenko, Y.; Rebane, A.; Wilson, C.; Screen, T.; Anderson, H. *J. Am. Chem. Soc.* **2006**, *128*, 12432–12433.
- Shoji, O.; Okada, S.; Satake, A.; Kobuke, Y. *J. Am. Chem. Soc.* **2005**, *127*, 2201.
- (a) Ohashi, A.; Satake, A.; Kobuke, Y. *Bull. Chem. Soc. Jpn.* **2004**, *77*, 365. (b) Ikeda, C.; Satake, A.; Kobuke, Y. *Org. Lett.* **2003**, *5*, 4935. (c) Hong, Y.; Dong, Y.; Tong, H.; Li, Z.; Haubler, M.; Lam, J. W. Y.; Tang, B. *Z. Proc. SPIE* **2007**, *6470*, T1–T12. (d) Ahn, T.; Kim, K.; Noh, S.; Aratani, K.; Ikeda, C.; Osuka, A.; Kim, D. *J. Am. Chem. Soc.* **2006**, *128*, 1700–1704.
- Birge, R. R.; Pierce, B. M. *J. Chem. Phys.* **1979**, *70*, 165.
- (a) Varnavski, O. P.; Ranasinghe, M.; Yan, X.; Bauer, C. A.; Chung, S.-J.; Perry, J. W.; Marder, S. R.; Goodson, T., III *J. Am. Chem. Soc.* **2006**, *128*, 10988–10989. (b) Ranasinghe, M. I.; Varnavski, O. P.; Pawlas, J.; Hauck, S. I.; Louie, J.; Hartwig, J. F.; Goodson, T., III *J. Am. Chem. Soc.* **2002**, *124*, 6520–6521.

JA804415B